Soriano Amat, M., Martins H.F., Durán, V., Martín López, S., González Herráez, M. & Fernández Ruiz, M.R. 2021, "Quadratic phase coding for SNR improvement in time-expanded phase-sensitive OTDR", Optics Letters, vol. 46, no. 17, pp. 4406-4409.

Available at http://dx.doi.org/10.1364/OL.432350

Quadratic phase coding for SNR improvement in time-expanded phase sensitive OTDR

MIGUEL SORIANO-AMAT,[1*] HUGO F. MARTINS, [2] VICENTE DURÁN, [3] SONIA MARTIN-LOPEZ, [1] MIGUEL GONZALEZ-HERRAEZ,[1] MARÍA R. FERNÁNDEZ-RUIZ[1]

[1]*Departamento de Electrónica, EPS, Universidad de Alcalá, 28805 Madrid, Spain*
[2]*Instituto de Óptica "Daza de Valdés" IO-CSIC, C/Serrano 121, 28006 Madrid, Spain*
[3]*Institut of New Imaging Technologies, GROC-UJI, 12071, Castellón, Spain*
**Corresponding author: miguel.soriano@uah.es*

Time-expanded phase-sensitive OTDR (TE-ΦOTDR) is a dual-comb-based distributed optical fiber sensing technique capable of providing centimeter scale resolution while maintaining a remarkably low (MHz) detection bandwidth. Random spectral phase coding of the dual combs involved in the fiber interrogation process has been proposed as a means of increasing the signal-to-noise ratio (SNR) of the sensor. In this letter, we present a specific spectral phase coding methodology capable of further enlarging the SNR of TE-ΦOTDR. This approach is based on the use of a quadratic spectral phase to precisely control the peak power of the comb signals. As a result, an SNR improvement of up to 8 dB has been experimentally attained with respect to that based on the random phase coding previously reported.

Optical fiber sensors based on Rayleigh scattering are increasingly gaining attention in the distributed sensing market due to the excellent performance attainable in terms of resolution, sensitivity, response time and sensing bandwidth with a relatively simple configuration [1-3]. In these sensors, an optical waveform is launched into the fiber under test (FUT) and Rayleigh backscattered light is detected and processed. From this signal, it is possible to localize and measure variations of physical magnitudes (such as temperature or strain) occurring in the neighborhood of the fiber. Both frequency and time domain approaches have been employed to interrogate the FUT and retrieve the sensing information.

Optical frequency-domain reflectometry (OFDR) usually employs a tunable laser source (TLS) for introducing a large frequency sweep into the fiber [1]. The attained spatial resolution depends on the scanned frequency bandwidth, delivering down to sub-millimeter spatial resolutions over measuring ranges of tens of meters [4]. For this purpose, stringent requirements are imposed on the TLS, which should be a fast-sweeping and highly stable source (i.e., without mode hops). In general, the frequency-domain interrogation imposes a relatively low acquisition sampling, constraining the use of OFDR in applications requiring real-time monitoring over relatively long fibers (i.e., hundreds of meters).

Among the time-domain approaches, phase-sensitive optical time-domain reflectometry (ΦOTDR) is a widely used technique that enables quantification of the perturbation surrounding the fiber, in contrast to incoherent OTDR. ΦOTDR systems have demonstrated to be a cost-effective tool for real-time monitoring of large structures such as pipelines and power cables, for the surveillance of security perimeters and for performing arrayed seismic measurements [2,3,5]. ΦOTDR offers a high measuring range (even more than 100 km when assisted by distributed amplification techniques [3]), real-time measurements and acoustic sampling only limited by the length of the fiber, although the spatial resolution is typically restrained to a few meters. In general, this resolution is limited by the width of the pulses launched to the optical fiber, which must be wide enough for the sensor to achieve a high signal-to-noise ratio (SNR). Note that the peak power of the pulse is limited by the onset of nonlinear effects. Spatial resolution in the centimeter scale has been achieved by using pulse coding strategies [6]. However, such high spatial resolution requires short pulses and, hence, a significant increase of the detection and acquisition bandwidths, along with the need of dealing with a high amount of data.

Very recently, we proposed a novel technique called time-expanded ΦOTDR (TE-ΦOTDR) [7]. It relies on the use of a dual frequency comb (DFC) to interrogate the optical fiber. In particular, one comb is launched to probe the fiber, while the second comb (identical to the first one but with slightly different repetition rate) is used as a local oscillator (LO). The result is a multi-heterodyne detection that efficiently down-converts the optical signal to the radio-frequency (RF) domain. In the time-domain, whenever the spectral phases of the two combs are the same, the process can be seen as a "time

expansion" of the detected optical traces. Then, low bandwidth electronics (in the MHz range) can be employed for acquiring an optical bandwidth of a few GHz, providing cm resolutions [7]. The dual combs are typically generated by electro-optic single-sideband modulation with carrier suppression implemented via intensity modulation and optical filtering. This procedure offers an extraordinary flexibility in the selection of the dual comb parameters, such as the optical bandwidth (associated with the sensor spatial resolution), the comb line spacing (linked to the attainable range) and the combs' line spacing offset (imposing the sensing sampling rate).

If the comb's spectral phase is flat (or, more generally, linear) (Fig. 1a), a train of short transform-limited pulses with high-peak power appears in time domain (Fig. 1b). Their peak-to-average power ratio (PAPR) can be approximated to BW/f_R, where f_R is the pulse repetition rate and BW is the optical bandwidth. These short pulses severely limit the energy efficiency of the interrogation module, as the average power of the waveform must be drastically reduced to avoid non-linearities in the modulation stage and along the FUT. In the original formulation of the technique [7], a random spectral phase distribution was allocated to the comb lines to prevent the formation of high peak-power pulses and reduce the PAPR (Fig. 1c). In particular, for the combs in [7], the PAPR is about 27 dB when considering the transform limited case, while it is reduced to 9 dB when the comb lines have a random spectral phase. However, although the power of the probe is distributed along the period of the signal, it has a speckle-like shape (Fig. 1d), and the PAPR is still high. In principle, this value could be further reduced by optimizing the random phase distribution. However, it would involve the employment of complex algorithms, implying heavy computational cost. Besides, the optimal phase may be different for different comb parameters, hampering the system tunability. In this letter, we propose the use of an alternative spectral coding able to further minimize the PAPR of the probe signal, bringing it down closer to 1 (0 dB). In particular, we propose the use of a quadratic spectral phase (Fig. 1e). Our hypothesis is that, under certain conditions over the bandwidth and line spacing of a rectangular-envelope frequency comb, it is possible to find a particular quadratic phase that implements a frequency-to-time mapping (far field condition) [9,10], in such a way that the temporal pulses have also a rectangular envelope whose full width coincides with the pulse train period. In that case, the PAPR of the temporal waveform would be close to 0 dB with a very simple phase profile with no need for heavy computational procedures. To formulate the described procedure, we start defining a transform limited optical frequency comb as a sequence of sinc-like pulses,

$$e_i(t) = A\cdot\mathrm{sinc}\left(tB_0\right) * \sum_{m=-\infty}^{\infty}\delta\left(t-m/f_R\right), \qquad [1]$$

where $*$ stands for convolution, A is the amplitude of the sinc-like pulses, B_0 is the comb optical bandwidth, and f_R is the comb line spacing. In spectral domain, the comb can be written as

$$E_i(f) \propto rect\left(\frac{f}{B_0}\right)\cdot\sum_{m=-N/2}^{N/2}\delta\left(f-m\cdot f_R\right) = \hat{E}_i(f)\cdot\sum_{m=-N/2}^{N/2}\delta\left(f-m\cdot f_R\right), \qquad [2]$$

where N is the number of lines and $\hat{E}_i(f)$ is the spectral envelope of the comb. Now, let us introduce a quadratic spectral phase modulation to the comb spectrum. The resulting field E_o is then given by

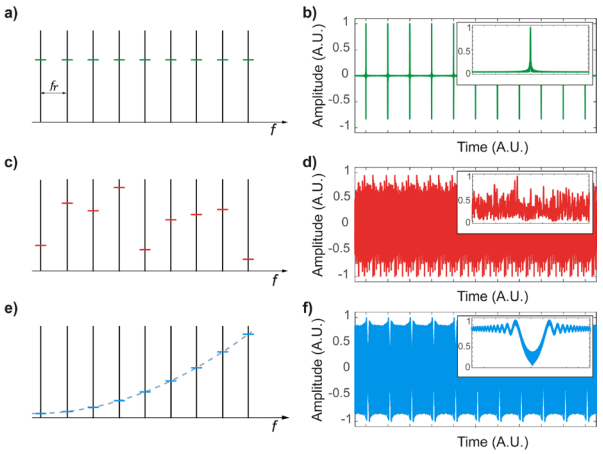

Fig. 1. Optical frequency comb (OFC) with flat spectral phase in frequency (a) and time domains (b). OFC with a random spectral phase modulation, in frequency (c) and time domains (d). OFC with a quadratic spectral phase, in frequency (e) and time domains (f). The insets of (b), (d) and (f) show a zoomed region of the modulus of the time-domain waveforms, where it can be seen how the PAPR is highly improved when the comb spectral phase has a quadratic modulation.

$$E_o(f) = E_i(f)\cdot\exp\left\{j\frac{\Psi(2\pi f)^2}{2}\right\}, \qquad [3]$$

where Ψ is the quadratic phase coefficient. In time domain, Eq. 3 can be written as

$$e_o(t) = \left[\hat{e}_i(t) * \sum_{m=-\infty}^{\infty}\delta\left(t-\frac{m}{f_R}\right)\right] * \exp\left\{-j\frac{t^2}{2\Psi}\right\}, \qquad [4]$$

being $\hat{e}_i(f)$ the IFT of $\hat{E}_i(f)$. Applying the associative property of convolution, and developing the integral convolution for one period

$$e_o(t) \propto \int\hat{e}_i(\tau)\exp\left[-j\frac{(t-\tau)^2}{2\Psi}\right]d\tau = \exp\left[-j\frac{t^2}{2\Psi}\right]\int\hat{e}_i(\tau)\exp\left[-j\frac{\tau^2}{2\Psi}\right]\exp\left[-j\frac{\tau t}{\Psi}\right]d\tau. \qquad [5]$$

being $t\in\left[(l-1)/f_R, l/f_R\right), l\in\mathbb{Z}$. If most of the pulse power is within a well-defined temporal window Δt, and it is accomplished that $\Delta t^2/(2\Psi) << \pi$ (temporal far-field condition), the first exponential factor within the integral can be neglected. The second exponential factor can be seen as the kernel of a Fourier transformation, so Eq. 5 can be simplified to

$$e_o(t) \propto \exp\left[-j\frac{t^2}{2\Psi}\right]\hat{E}_i(f'), \qquad [6]$$

where $f' = t/2\pi\Psi$. Hence, when the temporal far-field condition is accomplished, there is a frequency-to-time mapping and the temporal pulses have a rectangular-like shape (see Eq. 2) with a quadratic temporal phase. The width of the pulses, given by $2\pi\Psi B_0$, can be

controlled by the quadratic coefficient Ψ. If this width is intended to match the pulse train period, then Ψ is given by:

$$\Psi = \frac{1/f_R}{2\pi B_0}. \qquad [7]$$

In practice, the value of the quadratic coefficient that will provide the best result in terms of PAPR is not exactly that given by Eq. 7. The reason is that the tails of the pulses interfere even when the far field condition is satisfied in good approximation. This effect can be seen in Fig. 1f. Hence, the optimal quadratic phase coefficient will be slightly smaller than the theoretical one given by Eq. 7, although the exact value will depend on the comb's parameters (typically around 95% of the theoretical value). The temporal far-field condition can be expressed as a function of the optical bandwidth and line spacing of the comb by approximating $\Delta t \approx 1/B_0$ and substituting Ψ by its expression in Eq. 7. By doing some simple algebra, the far field condition can be expressed as $f_R << B_0$. This condition is accomplished as long as the optical frequency comb has a sufficiently high number of lines (e.g., > 10 lines), which is readily met in the broad majority of practical cases.

To demonstrate the performance improvement of the quadratic phase coding over that previously demonstrated by random phase coding, we have compared the sensing results obtained by TE-ΦOTDR with both coding strategies. For this purpose, we have measured a sinusoidal strain perturbation applied on the FUT with a frequency in the acoustic range (500 Hz). The designed DFCs have 500 lines that cover an optical bandwidth of 5 GHz. Hence, we can interrogate 500 individual sensing points with a spatial resolution of 2 cm over a range of 10 m (f_R = 10 MHz). Besides, two different comb line spacing offsets δf have been employed for each dual comb scheme, i.e., providing sensing sampling rates of 2 and 8 kHz, respectively. The setup employed in the experimental test is depicted in Fig. 2. The light emitted by a low phase noise continuous-wave laser (CWL) is employed to seed two intensity Mach Zehnder modulators (MZMs). The target dual combs are designed offline and are electrically generated by a two-channel arbitrary waveform generator (AWG), which drives each modulator, by using a dual side band (DSB) configuration [7]. For a fair comparison between the generated DFCs, the peak powers of all the involved combs are adjusted to have the same value, preventing nonlinear effects from appearing during the modulation and when the light propagates through optical amplifiers. The introduction of the parabolic spectral phase makes it possible to increase the average electrical power sent to each modulator in ~7 dB, reaching a PAPR of 2 dB. When compared with the transform limited case, this improvement reaches about 25 dB. In order to ensure an unambiguous down-conversion, one sideband of each DSB comb is removed by means of a tunable optical band pass filter (TBPF). Then, the probe comb is boosted by a high-power erbium-doped fiber amplifier (EDFA). The amplified spontaneous emission (ASE) introduced by the high-power EDFA is filtered out by a dense wavelength division multiplexer (DWDM). The probe is then launched into the FUT through an optical circulator (Circ.). The peak power of all the employed combs at the front end of the FUT is 23.8 dBm. The FUT has a length of 3.56 m, where a small section (2 cm) is mechanically perturbed by means of a shaker. The backscattered signal is boosted by another EDFA and again the ASE is filtered out by another TBPF. The LO comb is amplified prior to the removal of one sideband. Then, the

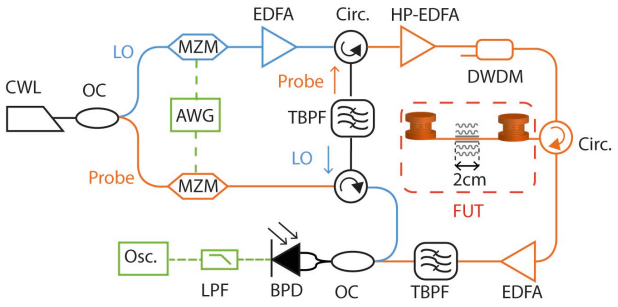

Fig. 2. Experimental setup. The probe and LO paths are distinguished by the orange and blue lines, respectively. The generation and detection stages in the electrical domain are pointed out in green. Acronyms are described in the text.

backscattered light is beaten with the LO. The interference is photodetected by a 100 MHz balanced photodetector (BPD), followed by an RF low pass filter (LPF) of 5 MHz to reduce noise. The resulting signal is digitized by an oscilloscope (Osc.) with 25 MHz sampling rate and digitally filtered after acquisition to restrict the measurement to the first Nyquist zone. Several polarization controllers and variable optical attenuators (not shown in Fig. 2) are placed along the setup for the signals to be properly conditioned.

The sinusoidal perturbation applied to the FUT is obtained via phase demodulation of the time-expanded (i.e., down-converted) traces, using a gauge length of 2 cm, which corresponds to the approximate width of the transform-limited pulses [7]. Fig. 3 shows the recovered strain map around the perturbed region for the 4 different DFCs. Fig. 3 a and b correspond to the combs with 2 kHz of acoustic sampling while Fig. 3 c and d correspond to the combs with 8 kHz of acoustic sampling. The left-hand side figures correspond to combs with quadratic spectral phase (the quadratic phase coefficient is $2.9918{\cdot}10^{-18}\,\mathrm{s}^2$), while those on the right-hand side correspond to the combs with random spectral phase. The phase in fading points is estimated based on nearest neighbor analysis [11]. As it can be seen in the figure, the DFC with quadratic phase modulation clearly offers measurements with better SNR, understood as the ratio between the perturbation power and the mean noise floor power in the PSD. As expected, the spatial resolution of the system is 2 cm. Also, the measurements obtained using lower sampling frequency have an improved performance. The reason lies in the down-conversion process performed by the dual comb configuration. Lower sampling frequency implies a longer temporal integration of traces, which is equivalent to perform an averaging process. As such, it is expected that an M-fold reduction in sampling frequency is associated with $\sqrt{M}$ increase in the SNR.

We have calculated the power spectral density (PSD) of the obtained perturbation curves to quantify the SNR improvement corresponding to (i) the newly proposed phase coding strategy and (ii) the different sampling frequency. The results are plotted in Fig. 4. In all cases, we observed a well-defined peak at the perturbation frequency (500 Hz). Few harmonics are also detected in multiples of this frequency, which may be explained by the non-linear response of the shaker. The measurements show a flat noise floor in all cases. The values of the noise floor and the peak power for different configurations are shown in Table 1. For the two sampling frequencies, the quadratic phase shows a noise floor substantially lower (~6 dB) compared to

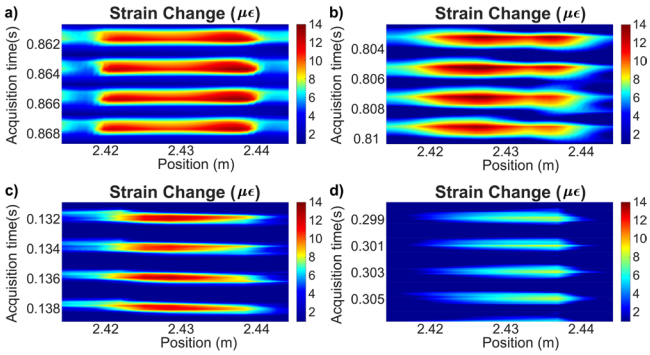

Fig. 3. Magnitude of the detected sinusoidal perturbation using a DFC with (a) δf =2 kHz and a quadratic phase modulation; (b) δf =2 kHz and a random phase modulation; (c) δf =8 kHz and a quadratic phase modulation; (d) δf =8 kHz and a random phase modulation.

the one obtained with the random phase. The values of the noise floor are obtained from the average of the PSD values between 750 and 850 Hz. According to Table 1, when compared to the random phase coding, the quadratic phase codification improves the SNR perturbation in 7 dB and 8 dB for sampling rates of 2 kHz and 8 kHz, respectively. The SNR improvement matches well with the reduction in the PAPR of the employed probes.

In conclusion, we have proposed a particular coding strategy to improve the energy efficiency of TE-ΦOTDR with minimal computational load. Considering a system using a rectangular-envelope DFC, we have proposed the use of a quadratic phase modulation capable of performing a frequency-to-time mapping that re-shapes the transform-limited sinc-like pulses

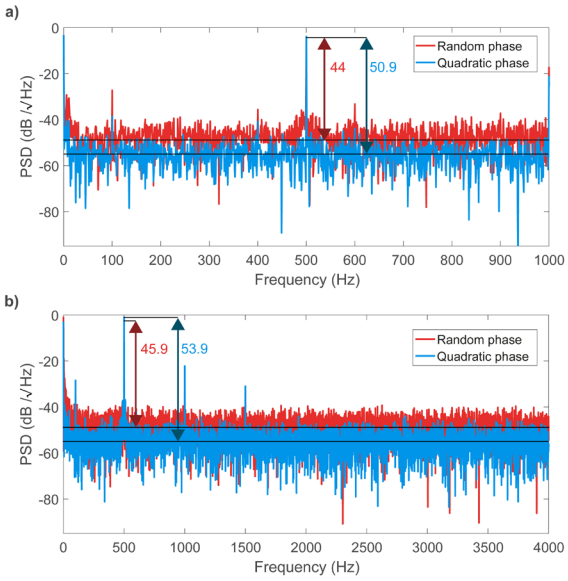

Fig. 4. Power spectral density (PSD) at the perturbed section of the FUT for a) 2kHz and b) 8 kHz of acoustic sampling. The results of using combs with random (quadratic) phase modulation are shown in red (blue).

Table 1. List of values for the noise floor and signal peaks for different codifications and acoustic samplings

	2 kHz		8 kHz	
	QP	RP	QP	RP
Signal peak $\left(\mathrm{dB}/\sqrt{\mathrm{Hz}}\right)$	-3.9	-4.3	-0.93	-2.8
Noise Floor $\left(\mathrm{dB}/\sqrt{\mathrm{Hz}}\right)$	-54.8	-48.3	-54.8	-48.7
SNR (dB)	50.9	44	53.9	45.9

QP: quadratic phase, RP: random phase.

into rectangular pulses whose width approximately coincides with the pulse train period. In this case, the PAPR of the resulting waveform is optimized, obtaining a value of about 2 dB (closer to the optimal case of PAPR = 0 dB). The use of a DFC configuration ensures that the detected signal is directly the impulse response of the fiber, with no need for complex, time-consuming decoding algorithms. Additionally, the DFC implies an efficient spectral down-conversion, delivering an extraordinary resolution of 2 cm with detection bandwidth below 5 MHz. In our experimental test, the use of a quadratic phase modulation has demonstrated to increase the SNR in 7-8 dB with respect to the initially proposed random phase modulation, considering probe waveforms with identical peak powers.

Funding. Comunidad de Madrid and FEDER Program (P2018/NMT-4326), Generalitat Valenciana (PROMETEO/2020 /029), the European Research Council (ERC-2019-POC-875302), the Spanish Government (RTI2018–097957-B-C31, RTI2018–097957-B-C32, and RTI2018–097957-B-C33), and Universitat Jaume I (UJI-B2019–45).

Acknowledgments. M.S.A., H.F.M., V.D., and M.R.F.R. acknowledge financial support from the Spanish MICINN under contract no. PRE-2019–087444, IJCI-2017–33856, RYC-2017–23668, and IJC2018–035684-I, respectively.

References

1. Z. Ding, C. Wang, K. Liu, J. Jiang, D. Yang, G. Pan, Z. Pu, and T. Liu, Sensors 18, 1072 (2018).
2. F. Peng, H. Wu, X.-H. Jia, Y.-J. Rao, Z.-N. Wang, and Z.-P. Peng, Opt. Express, 22, 13804 (2014).
3 H. F. Martins, S. Martin-Lopez, P. Corredera, J. D. Ania-Castañon, O. Frazao, and M. Gonzalez-Herraez, J. Lightw. Technol. 33, 2628 (2015).
4. M. Luo, J. Liu, C. Tang, X. Wang, T. Lan, and B. Kan, Opt. Express, 27, 35823 (2019).
5. Z. Zhan, Seismol. Res. Lett. 91, 1 (2019).
6. Z. Wang, B. Zhang, J. Xiong, Y. Fu, S. Lin, J. Jiang, Y. Chen, Y. Wu, Q. Meng, and Y. Rao, IEEE Internet Things J. 6, 6117 (2019).
7. M. Soriano-Amat, H. F. Martins, V. Durán, L. Costa, S. Martin-Lopez, M. Gonzalez-Herraez, and M. R. Fernández-Ruiz, Light Sci. Appl. 10, 51 (2021).
8. I. Coddington, N. Newbury, and W. Swann, Optica 3, 414 (2016).
9. V. Torres-Company, D.E. Leaird, and A.M. Weiner, Opt. Express, 19, 24718 (2011).
10. Y. Park, T.-J. Ahn, J.-C. Kieffer, and J. Azaña, Opt. Express 15, 4597 (2007)
11. G. Tu, M. Zhao, Z. Tang, K. Qian, and B. Yu, J. Ligthw. Technol., 38, 6691 (2020)

Full Reference List

1. Z. Ding, C. Wang, K. Liu, J. Jiang, D. Yang, G. Pan, Z. Pu, and T. Liu, “Distributed Optical Fiber Sensors Based on Optical Frequency Domain Reflectometry: A review,” Sensors 18,4, 1072, (2018), special issue on Optical Fiber Sensors 2017.
2. F. Peng, H. Wu, X.-H. Jia, Y.-J. Rao, Z.-N. Wang, and Z.-P. Peng, “Ultra-long high-sensitivity Φ-OTDR for high spatial resolution intrusion detection of pipelines,” Opt. Express, 22, 11, 13804-13810 (2014).
3. H. F. Martins, S. Martin-Lopez, P. Corredera, J. D. Ania-Castañon, O. Frazao, and M. Gonzalez-Herraez, “Distributed vibration sensing over 125 km with enhanced SNR using phi-OTDR over a URFL cavity,”J. Lightw. Technol. 33, 12, 2628-2632 (2015).
4. M. Luo, J. Liu, C. Tang, X. Wang, T. Lan, and B. Kan, “0.5 mm spatial resolution distributed fiber temperature and strain sensor with position-deviation compensation based on OFDR, ”Opt. Express, 27, 24, 35823-35829 (2019).
5. Z. Zhan, “Distributed Acoustic Sensing Turns Fiber-Optic Cables into Sensitive Seismic Antennas,” Seismol. Res. Lett. 91, 1, 1-15 (2019).
6. Z. Wang, B. Zhang, J. Xiong, Y. Fu, S. Lin, J. Jiang, Y. Chen, Y. Wu, Q. Meng, and Y. Rao, “Distributed Acoustic Sensing Based on Pulse-Coding Phase-Sensitive OTDR,” IEEE Internet Things J. 6, 4, 6117-6124 (2019).
7. M. Soriano-Amat, H. F. Martins, V. Durán, L. Costa, S. Martin-Lopez, M. Gonzalez-Herraez, and M. R. Fernández-Ruiz, “Time-expanded phase-sensitive optical time-domain reflectometry,” Light Sci. Appl. 10, 51, 1-12 (2021).
8. I. Coddington, N. Newbury, and W. Swann, “Dual-comb spectroscopy,” Optica 3, 4, 414–426 (2016).
9. V. Torres-Company, D.E. Leaird, and A.M. Weiner, "Dispersion requirements in coherent frequency-to-time mapping"Opt. Express, 19, 24, 24718-24729 (2011).
10. Y. Park, T.-J. Ahn, J.-C. Kieffer, and J. Azaña, “Optical frequency domain reflectometry based on real-time Fourier transformation,” Opt. Express 15, 8, 4597–4616 (2007)
11. G. Tu, M. Zhao, Z. Tang, K. Qian, and B. Yu, "Fading noise suppression in Φ-OTDR based on nearest neighbor analysis," J. Lightw. Technol., 38, 23, 6691-6698 (2020)